Published online 7 February 2013 *Nucleic Acids Research, 2013, Vol. 41, No. 6* ***3659–3672***
doi:10.1093/nar/gkt050

Structure–function relationships of two paralogous single-stranded DNA-binding proteins from *Streptomyces coelicolor*: implication of SsbB in chromosome segregation during sporulation

Tina Paradzik[1], Nives Ivic[2], Zelimira Filic[1], Babu A. Manjasetty[3], Paul Herron[4], Marija Luic[2] and Dusica Vujaklija[1,*]

[1]Division of Molecular Biology, Rudjer Boskovic Institute, Zagreb 10002, Croatia, [2]Division of Physical Chemistry, Rudjer Boskovic Institute, Zagreb 10002, Croatia, [3]European Molecular Biology Laboratory, Grenoble Outstation and Unit of Virus Host-Cell Interactions, UJF-EMBL-CNRS, Grenoble CEDEX 9, 3265, France and [4]Strathclyde Institute of Pharmacy and Biomedical Sciences, University of Strathclyde, Glasgow G4 0RE, UK

Received September 17, 2012; Revised January 10, 2013; Accepted January 11, 2013

ABSTRACT

The linear chromosome of *Streptomyces coelicolor* contains two paralogous *ssb* genes, *ssbA* and *ssbB*. Following mutational analysis, we concluded that *ssbA* is essential, whereas *ssbB* plays a key role in chromosome segregation during sporulation. In the *ssbB* mutant, ~30% of spores lacked DNA. The two *ssb* genes were expressed differently; in minimal medium, gene expression was prolonged for both genes and significantly upregulated for *ssbB*. The *ssbA* gene is transcribed as part of a polycistronic mRNA from two initiation sites, 163 bp and 75 bp upstream of the *rpsF* translational start codon. The *ssbB* gene is transcribed as a monocistronic mRNA, from an unusual promoter region, 73 bp upstream of the AUG codon. Distinctive DNA-binding affinities of single-stranded DNA-binding proteins monitored by tryptophan fluorescent quenching and electrophoretic mobility shift were observed. The crystal structure of SsbB at 1.7 Å resolution revealed a common OB-fold, lack of the clamp-like structure conserved in SsbA and previously unpublished S-S bridges between the A/B and C/D subunits. This is the first report of the determination of paralogous single-stranded DNA-binding protein structures from the same organism. Phylogenetic analysis revealed frequent duplication of *ssb* genes in Actinobacteria, whereas their strong retention suggests that they are involved in important cellular functions.

INTRODUCTION

Streptomyces species are multicellular bacteria that exhibit a complex developmental programme and undergo morphological differentiation. Development of streptomycetes is initiated by spore germination, hyphal growth and branching that leads to the formation of vegetative mycelium. From this mycelium, new branches grow into the air forming a lawn of aerial hyphae, which eventually generate long chains of unigenomic spores. Much current knowledge of streptomycetes is based on genetic and genomic studies of *Streptomyces coelicolor* M145 (1). The large, linear chromosome of this bacterium encodes 7825 ORFs with a large number of genes (12.3%) predicted to encode a regulatory proteins. In addition, genome analysis has revealed the distribution of different types of genes. Nearly all genes expected to be essential, such as those for cell division, replication, transcription, translation and the biosynthesis of important primary metabolites, are located in the core region. Exceptions to this rule are often duplicated genes (2). Amongst the latter group are two paralogous genes encoding single-stranded DNA-binding (SSBs) proteins.

SSB proteins, essential for cell survival, are found in all domains of life and in viruses (3). *Escherichia coli* SSB has been used extensively for several decades for studying protein structure–function relationships (4). SSB binds to single-stranded DNA (ssDNA) with high affinity in a sequence-independent manner, thus protecting ssDNA intermediates and disrupting unproductive secondary structures. During DNA replication, recombination and repair (5), SSBs interact with an array of chromosome

*To whom correspondence should be addressed. Tel: +385 1 4571 258; Fax: +385 1 4561 177; Email: vujaklij@irb.hr

maintenance proteins, mobilize them to the site of activity and often stimulate their activities (6,7).

The primary structures of SSB proteins display two distinct domains: an N-terminal domain containing a conserved oligonucleotide-oligosaccharide fold (OB-fold) responsible for ssDNA binding (8) and a C-terminal domain enriched in glycine and proline residues with acidic amino acids in a hexapeptide motif (D-D-D-I/L-P-F), which is important for protein interactions (9). Most bacterial SSBs function as homotetramers in which four OB-folds act together to bind to ssDNA. The crystal structure of SSB from *E. coli* was solved first (10), after which several crystal structures from other bacteria were described, among them an SSB from *S. coelicolor* (SsbA) (11). Two major binding modes of the SSB tetramer have been proposed. In the $(SSB)_{35}$ binding mode, two subunits of the *E. coli* tetramer bind to 35 nucleotides, whereas in the $(SSB)_{65}$ mode, all four subunits participate in binding to 65 nucleotides. It has been suggested that different binding modes may be used during different processes in DNA metabolism (12).

The biological role of paralogous SSB proteins in other bacteria is poorly studied. Transcriptional profiles of two *ssb* genes have been reported for *Bacillus subtilis*; in this naturally transformable bacterium, one SSB is essential, whereas the other participates in competence-related recombination (13). A division of labour between SsbA and SsbB during genetic recombination in *B. subtilis* was recently reported (14). In addition, differential binding properties of SsbA and SsbB from another naturally transformable bacterium, *Streptococcus pneumoniae*, were reported (15).

The biological roles of paralogous SSBs in streptomycetes have not been reported until now. In this study, we have found a new and unexpected role of paralogous SSB protein in chromosomal segregation during morphological differentiation. In branching vegetative hyphae, chromosome copies are not segregated, and septation occurs unevenly (16). Nutrient depletion triggers the development of aerial mycelium and the start of the reproductive phase. In the aerial hyphae, intensive chromosome replication occurs producing $\geq$50 non-segregated linear chromosomes (17). Transformation of sporogenic aerial hyphae into chains of mature unigenomic spores requires two synchronous processes: formation of sporulation septa and chromosome segregation (18,19). Although progress has been made, there are still substantial gaps in understanding how dozens of linear chromosomes that are dispersed along aerial hyphae condense and accurately segregate into the nascent pre-spore compartments. Several proteins, such as $FtsK_{SC}$, SMC, ParAB and ParJ, have been identified as contributing to chromosome organization and distribution during S*treptomyces* sporulation. Various *ftsK*$_{SC}$ mutants frequently have irregular DNA content owing to large terminal deletions of the chromosome (20). The *smc*/*ftsK*′-truncation alleles, produced 7–15% of spores lacking DNA, whereas a segregation defect of 24% was observed for a *smc*/*parB* mutant (21,22). Mutants lacking *parA*, *parB* or *parJ* produce 19, 24 and 8% of spores lacking DNA, respectively (23–25). In summary, various combinations of mutant genes still produced viable spores, albeit at reduced frequency, suggesting that additional genes are responsible for proper chromosome segregation.

In this study, we addressed the biological role of the paralogous *ssb* genes in *S. coelicolor*, *ssbA* and *ssbB* designated in UniProtKB as *ssb2* and *ssb1*, respectively. We asked what is the driving force leading to the retention of alternative *ssb* genes. We found an unknown role of SsbB in chromosome segregation during reproductive growth of *S. coelicolor*. Consistent with the proposed cellular function of SSBs, transcriptional analysis showed that transcription of *ssbB* is upregulated in the later stage of growth and in a minimal medium that usually triggers spore formation. In addition, the *ssbB* promoter displayed unusual organizational features that might be important for its activity. Solved 3D structure of SsbB showed a unique interconnection by two S-S bridges between the A/B and C/D subunits. This is the first example of solved crystal structures of two paralogous SSB proteins from the same organism.

MATERIALS AND METHODS

Bacterial strains, plasmids and primers

The bacterial strains, plasmids, cosmids and primers used during the course of this study are listed in the Supplementary Tables S1–S3.

Bacterial growth conditions

E. coli strains NM522, ET12567 and XL1-Blue were grown in Lauria Bertaini (LB) medium at 250 r.p.m. and 37°C, whereas strains BW25113 (pIJ790) and BT340 at 30°C until induction of temperature-sensitive genes. The expression of recombinant proteins was induced with 1 mM isopropyl-b-D-thiogalactopyranoside. *S. coelicolor* M145 was grown at 250 r.p.m. and 30°C in liquid complete regeneration medium (CRM) (26), R5 or minimal medium (MM) and on solid media: Mannitol soya flour (MS), Tryptic soy broth (TSB) (Difco™) and MM (27). Appropriate antibiotics were added at the following concentration: 100 μg/ml of ampicillin, 50 μg/ml of apramycin, 25 μg/ml of chloramphenicol, 50 μg/ml of kanamycin, 25 μg/ml of nalidixic acid or 50 μg/ml of hygromycin, when necessary.

Gene cloning, heterologous over-expression and protein purification

The *ssbA* gene (previously *ssb*) from *S. coelicolor* (NCBI, Gene ID 1099343) was cloned as described previously (28). This construct was used to prepare all other recombinant *ssbA* genes used in this study. A DNA sequence containing *ssbA* and its upstream regulatory elements (promoter and SD sequence; pssbA) was reconstructed in the pGEM®-T vector and designated pGEM-pssbA, as shown (Supplementary Figure S1). This plasmid was digested with HindIII, treated with Klenow fragment to make blunt ends and again digested with SpeI. The DNA fragment carrying the pssbA sequence was further subcloned into the *Eco*RV and SpeI sites of pMS82b. This construct, pMS-pssbA as shown in

Supplementary Figure S1, was used for the complementation experiment. The *ssbB* gene from *S. coelicolor* (NCBI, Gene ID: 1098117) was cloned into pQE-30 and labelled pQE-ssbB, using the same approach as described for *ssbA* (28).

For expression of the His-tagged *ssbB* gene in *S. coelicolor*, this gene was subcloned into pGEM-T using S6pANTF and S6pANTR primers (Supplementary Table S3). This construct, pGEM-ssbB, which contained the original *ssbB* ribosomal binding site, was digested with EcoRI and HindIII and ligated into pANT849 generating pANT-ssbB that was used for the transformation of *S. coelicolor* protoplasts.

To obtain a construct with a DNA sequence covering the promoter and *ssbB*, cloning was performed in the same way as for *ssbA*; for details, see Supplementary Figure S2. The construct pMS-pssbB was used for the complementation experiment. The *ssbBΔC* gene, lacking the last 37 aminoacids at the C-terminus was obtained by polymerase chain reaction (PCR) using SC-BF and SSB119 R primers (Supplementary Table S3) with *S. coelicolor* genomic DNA as a template. The amplified DNA fragment was cloned into the vector pQE as described for the *ssbA* and *ssbB* genes. In the next step, *ssbB* from the pGEM-pssbB construct was replaced by *ssbBΔC* at the BamHI and HindIII restriction sites (Supplementary Figure S2). The construct pssbBΔC was further sublcloned into pMS82, giving pMS-pssbBΔC. All constructs were verified by DNA sequencing.

Over-expression of the *ssb* genes cloned into pQE expression system was achieved in *E. coli* NM522 and in *S. coeli*color carrying pANT-ssbB. *S. coelicolor* was grown in MM (50 mL) for 48 h, mycelia was harvested by centrifugation, disrupted by sonication (4×30 s) and the suspension was centrifuged at 10 000*g* for 15 min to remove cell debris. Purification of His-tagged SsbB from cell-free extract was achieved by Ni-NTA resin (Qiagen), as reported previously (28). Fractions with purified protein were pooled, desalted on PD10 columns (GE Healthcare) and concentrated for microcrystallisation experiments to 17 mg/ml in 50 mM Tris–HCl (pH 7.0). Phosphate buffer (pH 6.9) was used for fluorimetric titration experiments. The proteins (50 ng/lane) were run on 12% sodium dodecyl sulphate–polyacrylamide gel electrophoresis (SDS-PAGE), and gel staining was performed with PhastGel® Blue R (Sigma). Western blot analysis as described previously (29) was performed with the anti-SsbB antibody obtained from Pineda, Anticörper-Service, Germany. Antibody binding was visualized with peroxidase-coupled anti-rabbit antibody and chemiluminescent detection (peroxidase ECL™ Primer Western Blotting Detection Reagent kit, GeHealthcare).

Gene disruptions and complementation

Gene disruption experiments were performed by allelic replacement with transposoed cosmids from a single gene transposon insertion cosmid library (30). Cosmids containing transposon Tn*5062* inside *ssbB* (6C07.1.c02, at 53rd aa) and *ssbA* (h24-1.E01, at 124 aa) were introduced into the ET12567 non-methylating *E. coli* strain containing the non-transmissible *oriT* mobilizing plasmid, pUZ8002. Following a previously described method (31), conjugation to *S. coelicolor* was performed. Exconjugants were selected for apramycin resistance and kanamycin sensitivity generating TSB01, and an allelic replacement by a double crossover recombination event was verified by PCR using primers complementary to the transposon cassette (EZR2 and EZL1) and *ssbB*. The disrupted *ssbB* gene was complemented by introducing an integrative vector, pMS82, carrying the pssbB construct (pMS-pssbB). This plasmid was introduced into *E. coli* ET12567(pUZ8002) and transferred by conjugation into *S. coelicolor*. Exconjugants were selected on hygromycin generating TSB01. PCR and specific primers (Supplementary Table S3) were used to confirm plasmid integration into the *S. coelicolor* chromosome at the $attB_{\Phi BT1}$ site.

REDIRECT PCR-targeting technology (31) was used to replace the entire coding region of *ssbA* by an apramycin (*aac(3)IV*) resistance cassette. A mutagenic cassette (*FRT-oriTaac(3)IV-FRT*) was PCR amplified using the primers SSBAkoF and SSBAkoR (Supplementary Table S3) and pIJ773 as a template. The PCR product was used to transform *E. coli* BW25113(pIJ790) containing cosmid SCH24. Recombination was induced with *L*-arabinose, and colonies carrying the recombinant cosmid were selected as described previously (31). After PCR and restriction verification, a cosmid designated cSA01 (Supplementary Table S1) was introduced by transformation into *E. coli* ET12567(pUZ8002) and transferred by conjugation into *S. coelicolor*. This cosmid, cSA01, was used to generate an in-frame 'scar' mutation at the position of the resistance cassette. This was achieved by introducing cSA01 into *E. coli* BT340 (harbouring pCP20 with the Flipase gene, FLP) in which temperature-induced recombination between both FRT mutagenesis cassette-flanking regions takes place. The resulting cosmid, cSA02, had an 81 bp 'scar' remaining in-frame with the adjacent ORF. This cosmid was used to transform *S. coelicolor* protoplasts carrying an additional copy of *ssbA* at the *att* $B_{\Phi BT1}$ site and the original *ssbA* locus. Kan^R recombinants were selected and re-streaked without kanamycin. The resulting colonies were again cultured for one generation with and without antibiotic to identify loss of kanamycin resistance, i.e. double crossing over. Selected colonies were checked for the presence of the 'scar' sequence instead of the *ssbA* gene by PCR using SSBAFRT and izaSSBA primers (Supplementary Table S3). In the original protocol, the unmarked 'scar' sequence was used for replacing the disruption cassette carrying the resistance gene (31). In our case, we applied the same approach to replace the undisrupted *ssbA*, as the disruption cassette in place of *ssbA* would not give any viable colonies.

Transcription analysis

Total RNA was isolated from *S. coelicolor* M145 grown in 50 ml of CRM (26) or MM liquid media (27). Sampling (3 ml) was performed at 18, 24, 48 and 96 h of bacterial growth followed by immediate RNA isolation with the

FastRNA® Pro Blue Kit and FastPrep® instrument (Qbiogene, Inc, CA) for 40 s at a speed setting of 6.0. Dnase I was used to remove remaining DNA. The quality of RNA was checked spectrophotometrically and by agarose gel electrophoresis, whereas the absence of DNA was confirmed by PCR.

Reverse transcription was performed using the High Capacity cDNA Reverse Transcription Kit (Applied Biosystems) with random hexanucleotides on 3 μg of total RNA isolated from each sample to examine expression of the *ssb* genes. Typically 2 μl of reaction volume with Complementary DNA (cDNA) and *ssb* primers, (Supplementary Table S3) were used for PCR. Amplified products were analysed by agarose gel electrophoresis.

Transcriptional start sites were determined by rapid amplification of cDNA ends (RACE) with the Invitrogen™ RACE kit according to the alternative protocol for first-strand cDNA synthesis of transcripts of high GC content. Three micrograms of total RNA from the exponential phase of growth (18 h) was reverse transcribed using SuperScript™ II RT and *ssb*-specific primers (Supplementary Table S3) or with MultiScribe™ Reverse Transcriptase (Applied Biosystems) according to the manufacturer's instructions. cDNA was purified using SNAP columns and C-tailed by terminal deoxyribonucleoside transferase (TdT). Two microlitres of this reaction mixture, *ssb* nested primers (Supplementary Table S3) and Abridged amplification primer were used for PCR. Non-tailed cDNA was used in PCR reactions as negative control. PCR products were separated, extracted from an agarose gel, cloned into vector pGEM-T (Promega) and sequenced to determine the transcriptional start site.

Fluorescence microscopy

For phase contrast and fluorescent microscopy, *S. coelicolor* M145, mutant strain, TSB01 and the mutant strain complemented with *ssbB* (TSB02) or with *ssbBΔC* (TSB03) were grown in the acute angle of sterile coverslips inserted obliquely in an MS plate. After 4 days, the coverslips were removed, and *in vivo* staining was performed immediately with DAPI (4′,6-diamidino-2-phenylindole) at a concentration of 1 μg/ml, whereas propidium iodide was used for visualization of fixed samples (32). Samples were studied using a Nikon TE2000S inverted microscope and observed with a CFI Plan Fluor DLL-100× oil N.A. 1.3 objective lens, and images were captured using a Hamamatsu Orca-285 Firewire digital charge-coupled device camera (33). Captured images were processed using IPlabs 3.7 image processing software (BD Biosciences Bioimaging, Rockville, MD). Statistical analyses of spores were performed using Statistica 8 (StatSoft Inc.).

Crystallisation and structure determination

Before crystallisation, the SsbB protein sample was centrifuged for 3 min at 10 000 r.p.m. Large hexagonal crystals were obtained in hanging drops consisting of 1 μl of protein solution (15 mg/ml), 1 μl of trypsin (0.01 mg/ml) and 1 μl of reservoir solution (0.2 M diammonium hydrogen citrate (pH 5.0), 20% (w/v) polyethylene glycol (PEG 3350) and 10% glycerol). Without addition of trypsin, no crystals were obtained. Mass spectrometry analysis showed that SsbB in the crystal was 116 aa long, indicating that trypsin digested 40 aa of the flexible C-terminus, allowing the protein to crystallize. A complete data set to 1.7 Å resolution was collected at BM14 beamline, ESRF (Grenoble, France) and processed using HKL2000 (34). The structure was solved by molecular replacement using the EPMR software (35) and SsbA (pdb code: 3EIV) as a starting model. Arp/Warp (36) was used for automatic model building and Coot for manual model building and real-space refinement (37). Restrained refinement was done using REFMAC5 (38). Crystallographic data collection and refinement statistics are shown in Supplementary Table S4. In the final model, there are 12 chains in the asymmetric unit. In chains *A*, *D*, *E*, *F*, *I* and *K*, all residues were built to fit the electron density (1–110). Chains *B*, *C*, *G*, *H*, *J* and *L* are missing some residues in the loop regions (*B*: 40–41, *C*: 40–43, 85–92, *G*: 39–44, 86–92, *H*: 42–43, *J*: 39–42, *L*: 40–42, 86–92).

Electrophoretic mobility shift assay

Formation of SsbA- or SsbB-ΦX174 DNA complexes were analysed by Electrophoretic mobility shift (EMSA). Various concentrations of SSB proteins were mixed with 7.7 nM of ssDNA in the reaction solutions containing 40 mM Tris acetate (pH 7.5), 10 mM $MgCl_2$ and 1 mM ethylenediaminetetraacetic acid in a total volume of 20 μl (Figure 7A1 and 2). To test the inhibitory effect of dithiothreitol (DTT), increasing amounts (10–100 mM) were added to the binding buffer (Supplementary Figure S7C). Mixtures were incubated 15 min at 37°C and then analysed on a 0.5% agarose gel.

Fluorescence measurements

Fluorometric titrations of Ssb protein solutions were performed on a Varian Cary Eclipse spectrofluorometer at room temperature using quartz cuvettes (1 cm), by excitation at a wavelength of 295 nm and emission monitored at 353 nm. Titrations were performed by titrating SSB proteins ($c_{monomer} = 6.9 \times 10^{-7}$ M) with small aliquots of dT_{35} stock solution ($c = 1.9 \times 10^{-5}$ M). After each addition, the solution was allowed to equilibrate for 5 min until no further change in fluorescence was observed. The fluorescence spectra were corrected for the buffer/NaCl baseline for each sample. The fluorometric titration data were analysed by non-linear fitting procedure to the Scatchard equation (39), to avoid large errors of linear processing of the fluorometric data (40).

Spore counting

Spore produced by M145 and TSB01 strains were counted using a Neubauer-improved haemocytometer (depth 0.02 mm). The spores were scraped with a microbiological loop from 3 spots of the same MS plate for each strain (~1/8 or 7 cm^2 of the plate). Spores were re-suspended in 1 ml of 0.1% Tween 80 (Sigma) and agitated vigorously with vortex mixer to disperse the clumps. The original spore suspension and 10^{-1} dilution of each sample were counted in the haemocytometer.

Spore resistance to heat and lysozyme

Heat resistance was assayed by incubating spores (10^6/mL) of the wild-type and *ssbB* mutant strain spores at 30°C and 60°C simultaneously. Five microlitres of the sample was taken every 10 min and spotted onto LB agar. To examine resistance to lysozyme, 10^4 spores of the wild-type and *ssbB* mutant strains were streaked in patches and 5 μg/10 μL of lysozyme was applied to LB agar plates. Plates were incubated for 3 days at 30°C before being photographed (41).

Phylogenetic analysis

Sequence similarity searches were performed with BLASTP, whereas comparison, sorting and multiple sequence alignments were obtained with Promals (42). Substitution modelling was completed using ProtTest (43). Construction of the phylogenetic tree was made by the maximum likelihood method using PhyML (44). An aLRT (45) was used to test branch support. Seaview (46) was used for statistical report and CorelDRAW® for graphic presentation of the results. Protein similarity searches with *S. coelicolor* SsbA against complete genome sequences from the phylum Actinobacteria were performed. Representative paralogous genes from each suborder of Actinobacteria were used to construct the phylogenetic tree.

RESULTS

Analysis of *ssb* genes

Both *ssbA* and *ssbB* are positioned in the central region of the chromosome (Figure 1) that is not exposed to frequent deletion events and where many essential genes are located (2). SCO3907 (*ssbA*) encodes a protein of 199 aa, whereas SCO2683 (*ssbB*) encodes a protein of 156 aa. The two SSB proteins share an overall 35% sequence identity, mostly conserved in the first 110 aa that contains the OB-fold ssDNA-binding domain. The C-terminal region (89 aa long) of SsbA is enriched in glycine (>50%), making it highly flexible and disordered. An acidic ^{194}DEPPF sequence, at the very end of this protein, is essential for interacting with proteins (6) or with the OB-fold (47). In SsbB, the C-terminus is reduced to 50 aa, and it lacks the acidic tail, which is highly conserved in all SSB sequences (6).

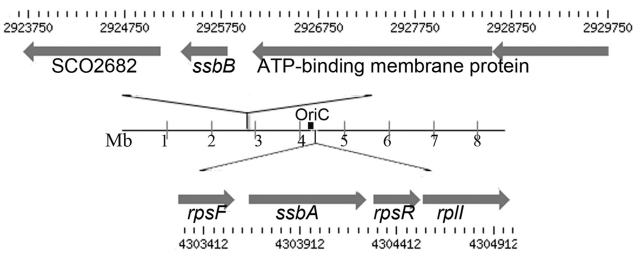

Figure 1. Physical map of *S. coelicolor* chromosomal region with two paralogous *ssb* genes. The gene *SCO3907* (*ssbA*) encoding a protein of 19.9 kDa is located 40 kb on the right side of the origin of replication (*oriC*), whereas the gene *SCO2683* (*ssbB*) encoding protein of 16.8 kDa is located 1.36 Mb on the left from the *oriC*. The both genes are positioned in a region that is not exposed to frequent deletion events and contains many essential genes.

Distinctive functions of paralogous SSBs

Retention of duplicate genes depends on their adoption of novel functions in the cell (48). To elucidate the biological role of SSBs in *S. coelicolor*, gene disruption experiments were performed as described in the 'Materials and Methods' section.

To disrupt *ssbA* by semi-targeted *in vitro* transposon mutagenesis, we introduced h24.EO1 (apramycin resistance—Apr^R, kanamycin resistance—Kan^R) by intergeneric conjugation and selected for Apr^R exconjugants. After screening 500 colonies for the Apr^R Kan^S phenotype indicative of integration of h24.EO1 by a double crossover event, all colonies displayed the Apr^R Kan^R, phenotype indicative of a single recombination event. The failure to obtain Apr^R Kan^S colonies suggests that either allelic exchange could not occur easily or that *ssbA* is an essential gene. As *ssbA* is clustered with genes encoding ribosomal proteins (*rpsF* and *rpsR*), a*s* in *B. subtilis* in which co-regulation of *ssbA* and ribosomal genes was reported (13), we created an in-frame deletion of *ssb*A to allow transcription of downstream gene(s). *S. coelicolor* was transformed with the cSA02 where *ssbA* was replaced by the 'scar mutation', and transformants were re-streaked without kanamycin. Single colonies were tested for the Kan^s phenotype indicative of a double recombination event, but none contained *ssbA* replaced by the 'scar' fragment. Deletion of *ssbA* was successful only when an additional copy of the gene was integrated into genome at the $attB_{\Phi BT1}$ site as described in 'Materials and Methods' section. In this case, we first selected for single-crossover mutants harbouring integrated cSA02 (Kan^R). All growing colonies were re-streaked without selective pressure. Finally, 100 colonies were tested for loss of Kan^R. Five sensitive colonies were verified for double crossing over by PCR. Two clones had the desired 'scar' mutation. Based on this result, we concluded that *ssbA* is essential for *S. coelicolor* survival.

To examine the biological role of *ssbB*, this gene was disrupted with Tn*5062*. Interestingly, after 4 days of growth, the mutant strain (TSB01) displayed white aerial mycelium on MS medium (Figure 2A). Formation of the white aerial hyphae [*whi* phenotype (49)] is characteristic of *Streptomyces* mutants that fail to develop grey pigment associated with mature spores. Further, we observed that after prolonged growth (10 days), the surface of our mutant turned light grey (Figure 2B), indicating that a small proportion of mutant hyphae could complete the spore maturation process. To exclude the possibility of an unpredicted polar mutation, the strain TSB01 lacking *ssbB* was complemented with the native gene integrated at the $attB_{\Phi BT1}$ site under the control of its own promoter. Strain TSB02, carrying this complementation vector, fully restored the original phenotype (Figure 2). Occasionally, TSB02 displayed darker grey pigmentation indicating higher production of spores. We speculate that this could be ascribed to *ssbB* chromosome relocation that consequently changed gene expression. To check

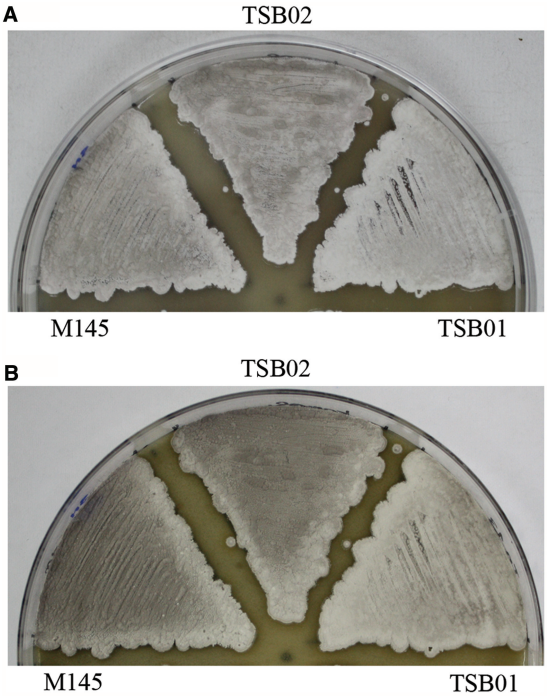

Figure 2. Phenotypes of the *ssbB* mutant (TSB01), complemented strain (TSB02) and their parental strain *S. coelicolor* M145. Strains were grown for at 30°C on solid MS media. TSB01 displayed a white phenotype on MS medium after 4 days (**A**) and light grey after 10 days of growth (**B**), whereas the phenotypes of parent strain and TSB02 were similar.

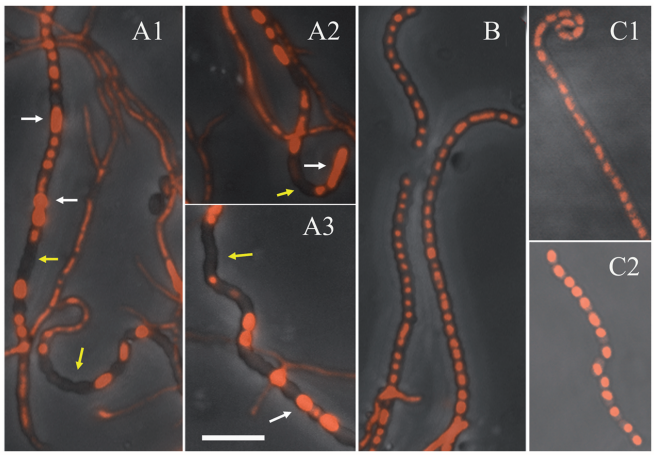

Figure 3. Phenotypic characterization by fluorescence microscopy revealed segregation defect in the strain lacking *ssbB*. Strains were grown on cover slips for 3 days and imaged with the fluorescence microscopy. The aberrant distribution of DNA is shown in spore chains of TSB01 (**A**1–3), whereas proper segregation can be seen in wild-type strain M145 (**B**), and TSB02 (**C**1 and 2). White arrows point to the spores with an excessive amount of DNA, whereas yellow to the compartment lacking DNA. Bar, 5 μm.

whether C-terminus of SsbB is important for DNA segregation during sporulation, we constructed TSB03 strain, i.e. mutant carrying *ssbBΔC* (see 'Materials and Methods' section); synthesis of SsbBΔC in TSB03 was confirmed by western blot (not shown). This strain also exhibited white phenotype as shown for TSB01 (Supplementary Figure S3A). Thus, this result confirmed that SsbB truncated at the C-terminus and with intact OB-fold could not restore spore maturation process. Both TSB01 and TSB03 displayed a similar phenotype on R5 medium. We observed a delay in formation of aerial mycelium and after prolonged incubation mutant colonies displayed a more pronounced pink colour (Supplementary Figure S3B) (50). Microscopy analysis also showed it was more difficult to find regions with abundant spore chains in TSB01. We performed simultaneous counting of the spores collected from the wild-type and TSB01, as described in 'Materials and Methods' section. The mean value of three independent counts for each strain showed that mutant strain produced 32.8% less spores than the wild-type strain. As shown in Figure 3A1–3, closer inspection showed that spores in the mutant strain frequently lacked DNA (30%; $n = 2200$) or contained excessive amounts of DNA (23%, $n = 900$), suggesting a defect in chromosome segregation. In contrast, the complemented strain (TSB02) displayed restoration of the wild-type phenotype (Figure 3C1 and 2), with just 1% of spores lacking DNA in TSB02 compared with the wild-type 0.8–1.1% of spores (21,25). To exclude the possibility that observed defect is an artifact because of the difficulty in stain penetration through the spore wall, we performed *in vivo* staining of the *S. coelicolor* wild-type, TSB01, TSB02 and TSB03 (Supplementary Figure S4). Staining with DAPI showed similar results as observed previously, in TSB01 25%, TSB03 26% and wild-type 1.5% of spores were deficient in DNA ($n = 800$). We further examined sensitivity of the spores for the wild-type strain and TSB01, by exposing them to moderate heat and lysozyme. Although both strains displayed the same sensitivity towards heat, TSB01 showed slightly higher sensitivity towards lysozyme (Supplementary Figure S5A and B). Statistical analysis showed that TSB01 had a slightly increased spore length and number of spores in spore chains (Table 1). The length of the spores in TSB01 was less uniform than in the wild-type, as can be seen from the standard deviation values. An F-test was also applied and showed that TSB01 spores were significantly longer than the wild-type strain ($P < 0.001$). The abberant distrubution of DNA in the spores and irregularly sized spores suggest that SsbB has a distinctive function for chromosome segregation (18). To the best of our knowledge, the role of an SSB protein in DNA partitioning was not previously reported. We also observed that the strain deficient in SsbB occasionaly produced longer and coiled aerial hyphae, (Suplementary Figure S6) as previously reported for the *whiA* mutant (51).

Expression profiles of *ssb* genes

The genetic evidence suggested that the *ssb* paralogs perform different biological roles: *ssbA* is essential for cell survival, whereas *ssbB* is important for production of viable spores. As the latter function is more pronounced at the end of the cell cycle, which correlates with nutrient depletion, we studied the effect of time and growth conditions on gene expression. *S. coelicolor* was grown in MM and CRM media for 4 days, and total RNA was isolated at different time intervals that coincided with metabolic

changes, as monitored by accumulation of actinorhodin, a red/blue acid/base indicator pigment with weak antibiotic properties (Figure 4C) (27). Reverse transcriptase (RT)-PCR analysis of *ssbA* indicated that this gene is expressed as a long mRNA with *rpsF* and most likely *rpsR* from a promoter positioned upstream of *rpsF*. Expression was more pronounced in the exponential phase of growth in rich medium (Figure 4A1), whereas in minimal medium (Figure 4A2), expression was prolonged into stationary phase. Under the same conditions, the *ssbB* transcript was hardly detectable in MM, whereas in rich medium, it was undetectable. Therefore, RT-PCR was extended to 35 cycles; even under modified condition, *ssbB* mRNA was barely detectable in rich medium. On the contrary, in minimal medium, the gene is expressed more or less equally throughout 96 h of growth (Figure 4B).

Table 1. Effect of the absence of *SsbB* in *S. coelicolor*

Variable	$\bar{x}\pm$ s[a] (95% CI)[b]		d[c]	*P-value*[e]
	M145	TSB01	(95% CI)[d]	
Number of spores in chain ($n = 100$)	27.20 ± 5.99 (25.50–28.90)	40.42 ± 13.6 (36.54–44.30)	13.22 (9.04–17.40)	<0.001
Spore length ($n = 200$)	1.24 ± 0.19 (1.21–1.28)	1.36 ± 0.35 (1.30–1.43)	0.12 (0.04–0.20)	<0.001

The mutant strain, TSB01, has an increased number of spores in spore chains and slightly increased spore length.
[a]Mean ± standard deviation.
[b]Lower and upper limit of the interval estimate for the mean with 95% confidence.
[c]d represents the difference between the means of wild-type and mutant data.
[d]Lower and upper limit of the interval estimate for d values in the population with 95% confidence.
[e]*P*-value obtained with *t*-test.

Identification of the promoter regions of *ssbA* and *ssbB*

As no obvious conserved promoter regions are present in the upstream regions of the two *ssb* genes, we analysed mRNA transcripts using 5′-RACE. As shown in Figure 4A, RT-PCR revealed that *ssbA* was transcribed as a long mRNA with ribosomal gene(s). Two primers, GSP1 located at the beginning of *ssbA* and RPR located at the end of *rpsF* (Figure 4) were used to obtain cDNA in a RACE experiment. Two transcriptional start points (TS1 and TS2) of *rpsF* were identified. TS1 was determined to be a G or C 75 nucleotides upstream of the start codon of *ssbA*, whereas TS2 was located 163 nucleotides upstream of the translational start codon of *rpsF*. By inspecting upstream regions of TS1 and TS2, we could not find obvious promoter consensus sequences. However, detailed analysis of the upstream region showed a TTTACT sequence, 6 nucleotides apart from the TS1 and a GAC motif 16 bp upstream of this sequence (Figure 5). These two putative promoter elements most closely resembled previously reported subclass G of *Streptomyces* promoters, GAC ($N_{18/19}$) T(N_4)T (52). Comparative analysis of these regions from other *Streptomyces* genomes displayed genetic variation upstream of the TS1 owing to short insertion and deletion events. Therefore, despite the synteny, the proposed promoter elements of the proximal promoter are located in the poorly conserved DNA region. The sequence homology blocks were found upstream of the TS2 (not shown). The sequence TACGCT, 6 nucleotides apart from the TS2, might act as a −10 consensus sequence [4 of **TA**g(**Pu**)(Pu)**T,** (53)], whereas sequence T TTCAA spaced 18 bp from the proposed −10 sequence might act as a −35 consensus sequence [4 of **TTGAC**(**Pu**), (53)]. We could not detect other transcriptional start in the intergenic regon (81 bp) of *rpsF* and *ssbA*.

The transcriptional start of *ssbB* was determined to be a C, 73 nucleotides upstream of the AUG codon. Analysis

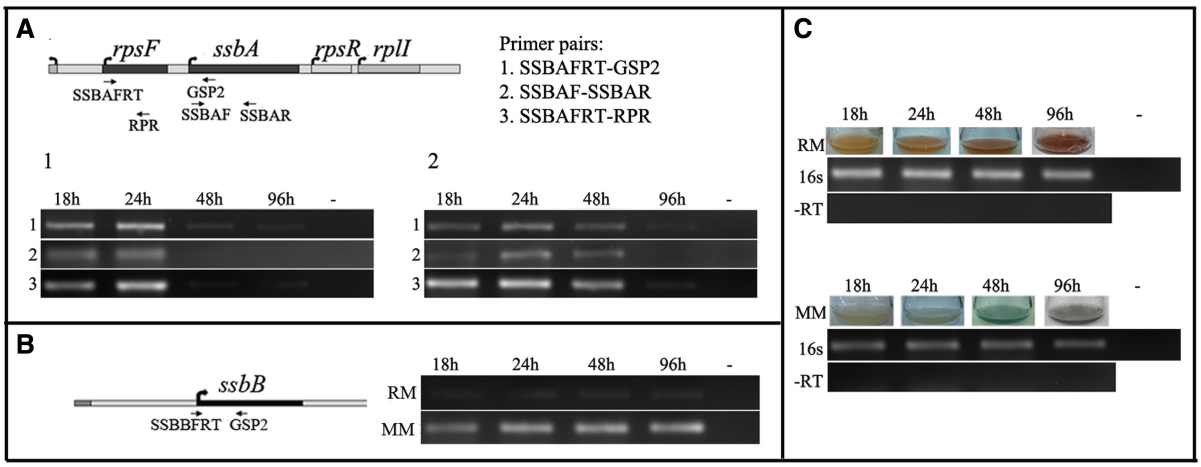

Figure 4. Expression profiles of *ssb* genes. Samples were taken at different stages of growth characterized by visible actinorhodin accumulation. Gene expression was analysed by RT-PCR as described in 'Materials and Methods' section. Total cDNA was obtained using random hexanucleotide primers, and PCR was performed with gene-specific primers positioned as indicated in (**A**) and (**B**). (A1) Expression of *ssbA* in rich media (RM), (A2) expression of *ssbA* in minimal media (MM). (B) expression of *ssbB* gene in RM and MM. (**C**) Control reactions and *S. coelicolor* culture flasks at given times, 16 s—upper panel shows expression of 16S rRNA in RM, whereas 16 s—lower panel in MM, -RT shows control reactions without reverse transcriptase.

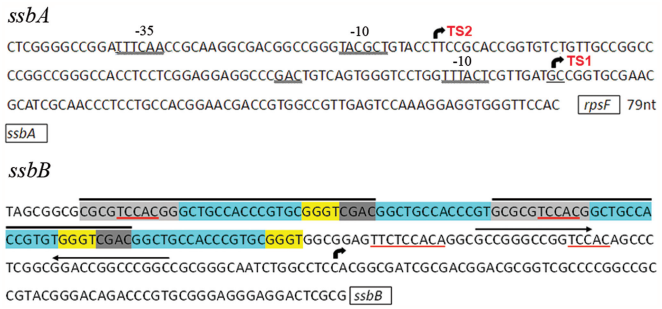

Figure 5. Transcriptional start sites of two *ssb* genes. The results of RACE experiment revealed that the transcription of *ssbA* gene starts at 75 bp (TS1) and 163 bp (TS2) upstream of *rpsF* gene (indicated by rightwards arrows). Also, −10 consensus sequence and −35 consensus sequence are underlined. Proposed promoter elements upstream of TS2 most closely resemble SEP-like sequences [TTGACPu-18- TAgPuPuT (53)].The transcription start site for *ssbB* gene is 73 nucleotides upstream of start codon (indicated by rightwards arrow). Promoter region of *ssbB* contains a palindromic sequence (opposite directed arrows), Dna box (red underline) and two long imperfect direct repeats (black overline), whereas identical shorter repeats are labelled in the same colour.

of the *ssbB* promoter region did not show typical *Streptomyces-E. coli* like, promoter sequence [**SEP**-like sequences; TTGACA-18bp-TCTTAT (54) and TTGAC Pu-18- TAgPuPuT (53)], although we observed its activity in *E. coli* (unpublished data). Detailed inspection showed a complex DNA region with a palindromic sequence, DnaA box and two long imperfect direct repeats as indicated in Figure 5. Moreover, part of this long repeat (GGCTGCCACCCGTGC) was found at three additional positions in this promoter region.

Determination of SsbB crystal structure and comparison with SsbA

We determined the crystal structure of a tryptic SsbB fragment (1–116 aa) lacking the structurally disordered C-terminus at 1.7 Å resolution. There are 12 copies of the SsbB monomer in the asymmetric unit, forming three homotetramers. The r.m.s. deviation of Cα atoms between SsbB tetramers is 0.6 Å [calculated using the SUPERPOSE programme from the CCP4 suite (55)]. Each SsbB monomer possesses a single OB-fold comprising five β strands forming a β barrel capped by an α helix and one additional β strand. One feature unique to SsbB is the presence of two intermolecular disulphide bonds between the Cys7 residues from the AB and CD subunits (Figure 6). The presence of S-S bridges was detected by sodium dodecyl sulphate–polyacrylamide gel electrophoresis or western blot (Supplementary Figure S7A and B) using SsbB purified from *S. coelicolor* and *E. coli* cells. The specificity of protein band at the expected position of SsbB dimer was confirmed by western blotting. The dimer structure of SsbB was disrupted on additon of DTT (100 mM). In addition, we showed that 10 mM DTT almost completely abolished SsbB binding to ssDNA, whereas affinity binding of SsbA was not changed even in the presence of 100 mM DTT (Supplementary Figure S7C). According to PISA server calculations (56), the free energy of the tetramer

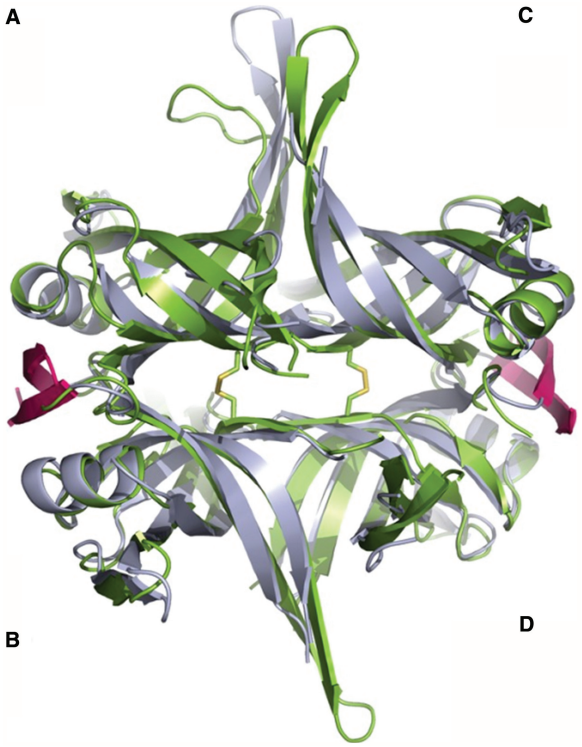

Figure 6. A superposition of SsbB (green) and SsbA (grey) structures. The monomers are designated (**A**), (**B**), (**C**) and (**D**) as shown. 3D structure of SSB proteins displayed similar structure with some unique variations. Disulphide bridges of SsbB are shown as yellow sticks, whereas the clamp structure of SsbA is in pink colour.

dissociation (ΔG^{diss}) for the entire SsbB tetramer is 19.5 kcal mol^{-1} (average value for the three tetramers), whereas for SsbA, this value is 11.7 kcal mol−1. Superposition of the quaternary structures of SsbA and SsbB from *S. coelicolor* is shown in Figure 6. The r.m.s. deviation of Cα atoms between SsbB and SsbA is 1.4 Å for entire tetramers and 1.0 Å for the superimposed monomers. The rotation of the BD subunit with respect to the AC subunit remains the same in both SsbA and SsbB (Figure 6).

Binding properties of paralogous SSB proteins

Cooperative binding mode of SSB proteins is important for DNA replication (6). To reinforce our finding that SsbA plays an important role during DNA replication, we evaluated the binding efficiency of SsbA and SsbB to the long ssDNA fragment by EMSA. Binding was tested using the circular ssDNA of Φ1748 (5386 nt). When increasing concentrations of SSB proteins were incubated with a fixed concentration of Φ1748 DNA, as described in 'Materials and Methods' section, a progressive decrease in the mobility of circular ssDNA could be seen for both proteins (Figure 7A1). However, a moderate concentration of salt (100 mM NaCl) significantly reduced cooperative binding of SsbB (Figure 7A2).

The ssDNA binding activity of SsbA and SsbB was also determined by fluorescence titration. Fluorescence titrations used to monitor the quenching of SSB tryptophans

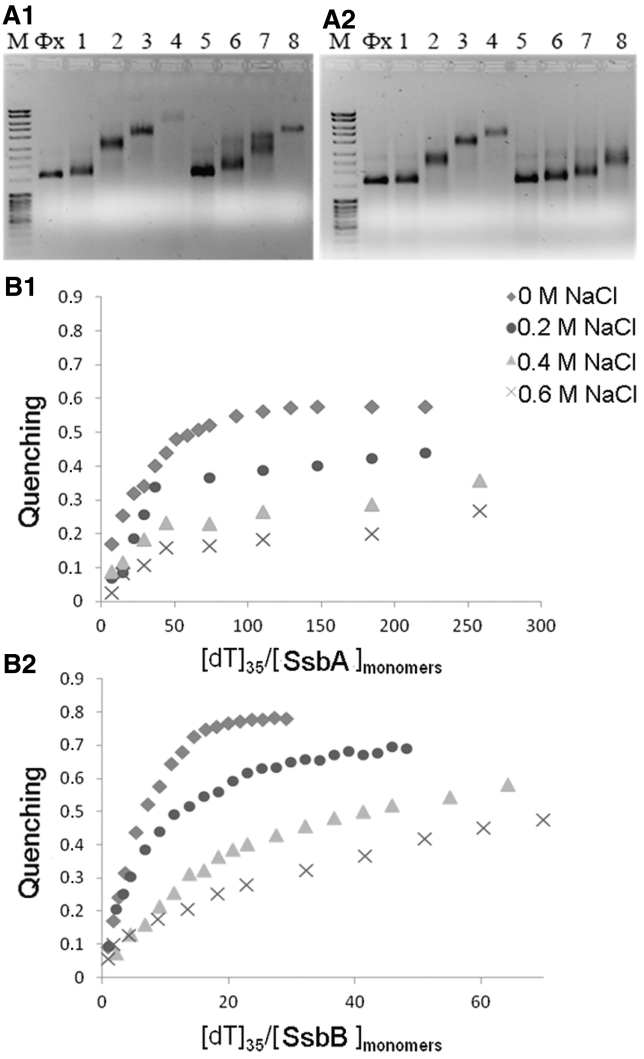

Figure 7. Electrophoretic mobility shift assays and fluorescent titrations. (**A**) Binding of SSB proteins to ΦX174 DNA was examined by EMSA. (1) Binding affinity without salt or (2) with 100 mM NaCl added to the reaction mixture. Lanes 1–4 contained SsbA protein at the following concentrations: 0.25 μM, 1.25 μM, 2.5 μM and 5 μM; lanes 5–8 contained SsbB with following concentrations: 0.25 μM, 1.25 μM, 2.5 μM and 5 μM. (**B**) Tryptophan fluorescent quenching of SsbA (1) and SsbB (2) while binding to dT_{35} at different salt concentrations, as indicated, were measured spectrophometrically as described in 'Materials and Methods' section.

on addition of dT_{35} showed that the binding affinities for both SSB proteins dropped significantly with the addition of NaCl (Figure 7B1 and 2). Furthermore, without salt, the binding constant (K_{35}) of SsbA is $7.9 \times 10^6\,M^{-1}$, whereas (K_{35}) of SsbB is $6.3 \times 10^7\,M^{-1}$, showing that SsbB binds to ssDNA dT_{35} at almost tenfold higher affinity.

Phylogenetic analysis of SSB proteins from Actinobacteria

Our results clearly show that two paralogous genes have adopted different cellular functions through evolution. We determined whether this duplication is common to other members of the same phylum. To gain a better insight into the phylogenetic relationships of SSB proteins, we collected and analysed 129 available SSB sequences from 60 genera of Actinobacteria. We found that ~90% of the analysed species possess at least two *ssb* genes. Representative paralogous genes from each suborder belonging to five orders of Actinobacteria, and two paralogous SSBs from *B. subtilis* as an outgroup, were used to construct a maximum likelihood tree. Our phylogenetic analysis (Figure 8) demonstrated that SsbB and SsbA are clustered separately within the orders Actinomycetales and Bifidobacteriales. Branch lengths indicate that cluster with *S. coeliclor* SsbB protein are more heterogeneous than cluster with SsbA, perhaps indicative of the essentiality of that cluster of proteins. Two species with three SSBs (*Stackebrandtia nausensis* and *Corynebacterium glutamicum)* were also included in the analysis. As shown (Figure 8), their SsbC proteins were clustered differently; *C. glutamicum* SsbC was clustered with the SSB-A group, whereas SsbC from *S. nausensis* was positioned separately. Orders Coriobacteriales, Rubrobacterales and Salinibrobacterales are branched together with high confidence (see aLRT values at nodes); however, their SsbB proteins, when present, do not form a separate cluster. As an outgroup, the two SSBs from *B. subtilis* (14) were grouped together.

DISCUSSION

Until now, two limited studies were performed on SsbA, reporting close structural similarities to mycobacterial SSBs (11,57) as well as tyrosine phosphorylation (28). *S. coelicolor* possesses two *ssb* genes; both genes are located in the core region of the linear chromosome of *S. coelicolor* (Figure 1) defined by the presence of essential genes (2). We hypothesized that the retention of a duplicate *ssb* gene might be associated with an important cellular function (48).

S. coelicolor survives without SsbB but displays defect in chromosome segregation during sporulation

Mutational analysis allowed new insight into the biological role of SsbA and SsbB. As described in 'Results' section, we failed to disrupt *ssbA* with Tn*5062*. This gene lies between *rpsF* and *rpsR*, encoding ribosomal proteins. Conserved synteny of these genes in distantly related bacteria and coupled transcription were reported previously (13). Therefore, a polar effect caused by insertional gene replacement was anticipated, and a 'scar' mutation at the *ssbA* locus was constructed. Despite this strategy, deletion of the *ssbA* locus was obtained only in a strain with an additional copy of the wild-type gene, indicating that *ssbA* is essential for *S. coelicolor* survival, in line with other bacteria (4,6,13). In contrast, the flanking regions of *ssbB* with neighbouring genes are >200 bp, and a polar effect was not anticipated. The *ssbB* gene was disrupted by replacing the original chromosomal sequence with an *S. coelicolor* mutagenized cosmid. Numerous recombinant colonies were obtained, indicating that this gene is not essential.

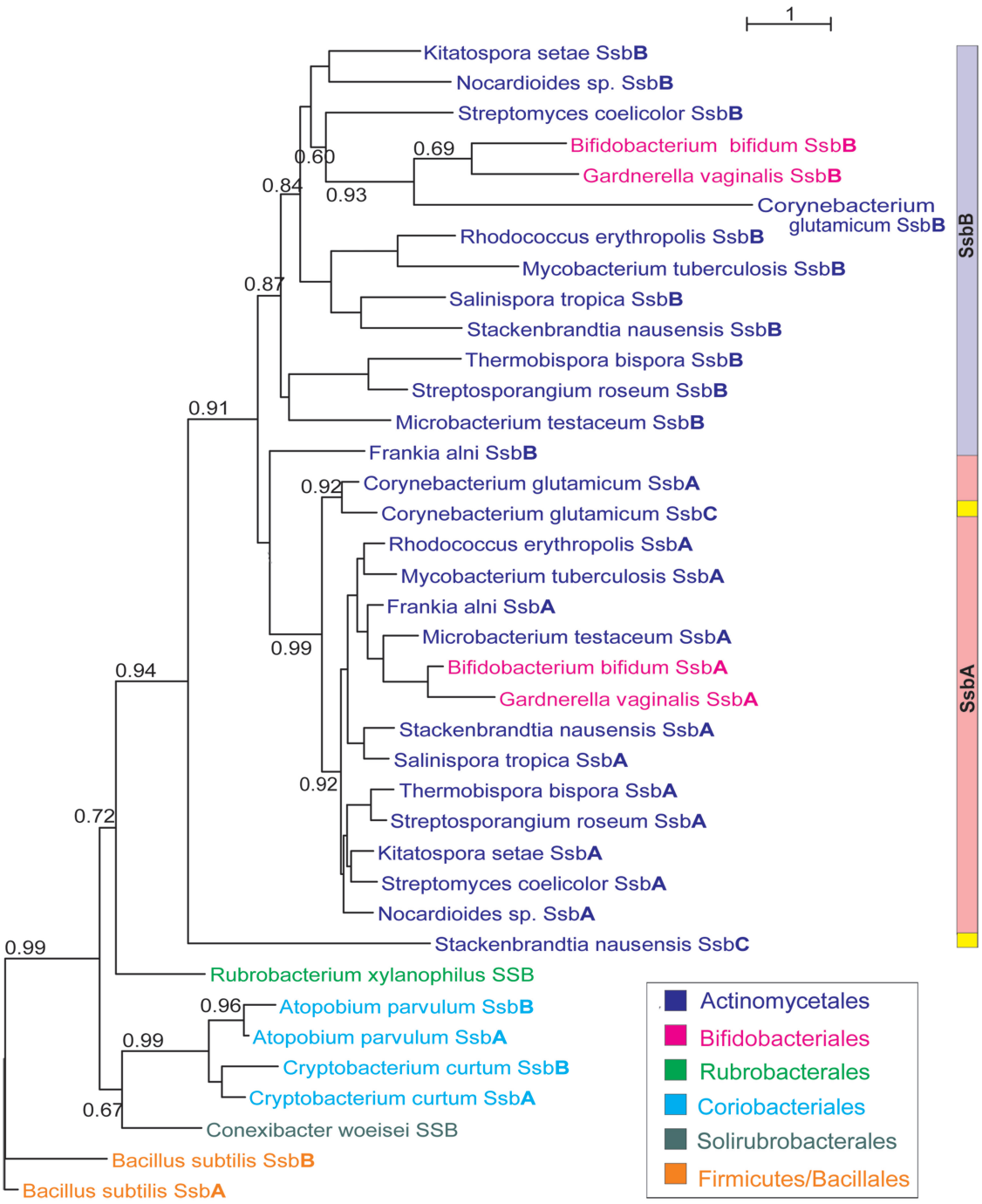

Figure 8. Phylogenetic tree of SSB proteins based on multiple alignment of full-length protein sequences from phylum Actinobacteria. The representatives of different orders are coloured as shown in legend, and aLRT values are shown for main branches.

However, the *ssbB* mutant (TSB01) displayed a white phenotype (Figure 2, Supplementary Figure S3A) and, although TSB01 differentiated on solid agar plates to form aerial hyphae, did not exibit the grey colour characteristic of mature spores. As we could restore the parental phenotype by introducing an additional copy of *ssbB* (Figure 2, strain TSB02), we concluded that the white phenotype was a consequence of the mutation in *ssbB*. This was unexpected and intriguing, as a role of SSB in morphological development had not been reported previously. A white phenotype is often associated with pleiotropic developmental regulators (18,58). Several mutants displaying this phenotype have been studied for decades. Genes blocked at early stages (*whiG*, *–A*, *–B*, *–H* and *–I*) are defective in sporulation septation, whereas *whiD* and *whiE* mutants are blocked in spore maturation (59). In addition, two mutants that belong to the SsgA-like proteins (SALP family), *ssgA* and *ssgB*, also display a non-sporulating white phenotype, whereas *ssgG* showed, after 6 days of growth, a light grey appearance similar to

the *ssbB* mutant (58). However, in this mutant, the unusually large spores, three to four times normal size, with proportionally segregated chromosomes were detected (58). As shown in Figure 3 and Supplementary Figure S4, the *ssbB* mutant produced spore chains with a severe nucleoid segregation defect. Unequal distribution of DNA in spore chains showed that the *ssbB* mutant was impaired in the segregation process rather than in replication. The percentage of spores lacking DNA in analysed spore chains was ~30%. This is higher than for mutants in other genes associated with chromosome segregation (22,23,25). At present, it is not easy to conclude by what mechanism SsbB participates in chromosomal partitioning. Complementation with a truncated *ssbB*, gene encoding protein with preserved tetramer structure, demonstrated that C-terminus of SsbB is important for its activity during chromosome segregation. Thus, we speculate that SsbB interacts and supports the function of other DNA-binding proteins known to be important for chromosomal segregation. For example, ParB binds to numerous *parS* sites near *oriC*, whereas ParA provides support for proper distribution of these nucleoprotein complexes (49). FtsK controls the partitioning of chromosome before septal closure (20), whereas SMC binds to DNA and promotes its condensation (22). Single, double and triple mutations of these genes (21) did not completely block nucleoid segregation during sporulation; moreover, the percentage of spores lacking DNA in analysed spore chains was <25%. This indicates that SsbB makes an important contribution to chromosome segregation during sporulation.

Our analysis (Table 1) showed that the *ssbB* mutant had an increased number of spores in spore chains and slightly increased spore length. Although sensitivity test towards heat and lysozyme did not show significant differences between wild-type strain and mutant (Supplementary Figure S5), major changes in spore wall morphology were anticipated, and it is next task to examine this in detail. It was previously reported that strains with a DNA segregation defect caused by *smc*, *ftsK* or *parB* mutations produced spores that were similar in shape and size to the wild-type strain (21). Contrary to the *smc*, *ftsK* and *parB* mutants, the *ssbB* mutant also displayed a white phenotype, and we hypothesize that our observation are due to more severe chromosome partitioning defect than those reported previously or that the *ssbB* mutation causes a distinct defect at a final stage of spore maturation. In any case, it will be a key challenge to clarify the role of the SsbB protein in the complex mechanism of cell division in *Streptomyces*.

Transcriptional profile of *ssb* genes correlates with their proposed biological functions

Differences in the transcriptional profile of *ssb* genes were in agreement with their proposed biological functions. The *ssbA* is expressed throughout bacterial growth, being significantly upregulated in rich medium during the logarithmic phase, whereas under starvation conditions, its expression is prolonged (Figure 4A2). This result corresponds to the cellular level of SsbA from *B. subtilis*, which is higher during intensive DNA replication in fast-growing vegetative hyphae (13) and indicates that *S. coelicolor* SsbA might be a crucial component of DNA metabolism. Prolonged transcription of *ssbA* in minimal medium could be correlated to nutrient-limiting conditions that trigger aerial mycelium formation. This consequently leads to intensive replication in the apical regions of hyphae (17). Transcriptional analysis clearly showed that *ssbA* is expressed at a much higher level than *ssbB* as reported for *B. subtilis* (13). Even when PCR was extended to 35 cycles, *ssbB* transcripts were barely detectable in rich medium, whereas in minimal medium, the gene is expressed more or less equally throughout 96 h of growth (Figure 4B). This is consistent with the proposed role of SsbB during reproductive stage of *Streptomyces* growth.

We also identified transcriptional start sites for *ssbA* and *ssbB* (Figure 5), and these results were in concert with the transcriptional starts identified independently by RNAseq (Dr. K. McDowall, personal communication). Although *ssbA* is transcribed throughout growth, the proposed proximal promoter region is more active (Dr. K. McDowall, personal communication) and does not display a typical *Streptomyces* vegetative σ factor consensus sequence. In contrary, the proposed distal promoter elements most closely resemble SEP-like promoters (53,54). By inspecting promoter regions of *ssbA*, we found only short motifs that partially resembled previously described regulatory elements (54). Altogether this is not surprising, as streptomyces promoter regions are poorly understood and highly divergent (52–54) owing to their numerous σ factors encoded by these organisms (2). The promoter region of *ssbB* is complex and unusual. It is extremely GC rich (78.9%) in comparison with average GC content of *Streptomyces* promoter regions estimated to be 57–62% (53). It also possesses various repeats and palindrome sequences as shown in Figure 5. We speculate that this may indicate interactions of the promoter region with DNA-regulatory protein(s) required for the tight regulation of *ssbB* expression. A similar expression profile and possible promoter regulatory elements are found in other genes involved in chromosome segregation. For example, the gene-proximal promoter (P1), governing the expression of *parAB* throughout growth on minimal medium, displays a similar pattern of activity to *ssbB*, whereas the gene-distal promoter (P2) is upregulated during spore chain formation (23).

Unexpectedly, the *ssbB* promoter was active in *E. coli* causing filamentous growth (data not shown), as reported previously (4). At present, it is difficult to explain how an extremely GC-rich sequence and no obvious SEP-like promoter could act as a regulatory element in a distantly related bacterium.

Crystal structure of SsbB revealed unique variations

This is the first example of solved crystal structures of two SSBs from the same organism. Although the quaternary structure of SsbB reported here highly resembles the quaternary structure of *S. coelicolor* SsbA (12), distinctive variations were observed. The clamp mechanism found

in SsbA, which includes a conserved ATAKVTK sequence (Figure 6) characteristic of high GC Gram-positive bacteria, is not preserved in SsbB. It has been proposed that this structure contributes to the stability of the SsbA homotetramer that is possibly important for the special requirement of high-GC content genomes (11). Therefore, we propose here that in the SsbB structure, this clamp is functionally substituted by two disulphide bridges that keep the quaternary structure highly stable and rigid. The presence of disulphide bridges in SSB structures has not been previously reported. As shown in Supplementary Figure S7A and B, disulphide bonds were detected in SsbB protein samples isolated from homologous and heterologous hosts. Although we could not exclude the possibility that S-S bond formation had occurred during protein purification, our results clearly indicated that binding affinity had decreased significantly in the presence of DTT (Supplementary Figure S7C). At present, we speculate that binding activity of the SsbB might be regulated during oxidative stress in *S. coelicolor*, and that formation of disulphide bridges increases its binding activity (60). In addition, calculations of the free energy of the tetramer dissociation (ΔG^{diss}) showed that SsbB is the most stable of all bacterial SSB proteins described so far (11).

SsbA and SsbB bind to ssDNA with different affinity

The EMSA experiment showed that SsbA and SsbB form complexes with circular ΦX1748 ssDNA. The results of this binding experiment indicated that SsbA binds to long ssDNA in a more cooperative way, as reported for SsbA from *S. pneumoniae* and SSB from *E. coli* (15,61). In addition, cooperative binding of *E. coli* SSB is favoured at low salt concentrations (61). The cooperative binding mode has been proposed to function in DNA replication (6). In agreement with this, our results support the predicted biological role of SsbA. Cooperative binding of SsbB was less pronounced and almost completely abolished under moderate salt concentrations (Figure 7A).

Different ssDNA binding affinities to dT_{35} were also observed for paralogous SSBs. Similarly to SSBs from *S. pneumoniae* (15), SsbB displayed a higher affinity for binding to shorter oligomers (dT_{35}) than SsbA (Figure 7B). Interestingly, the opposite result was published recently for SsbA and SsbB from *B. subtilis* (14). This discrepancy can be explained by differences in the C-terminal domain. Previous studies showed that the size of C-terminal region as well as conserved acidic tail play an important role in binding affinity (47,62). At present, we speculate that different binding properties of *S. coelicolor* SSB proteins might be a consequence of their biological functions.

Phylogenetic analysis indicates frequent duplication and retention of *ssb* genes in Actinobacteria

Our results show that two paralogous genes have adopted different biological functions through evolution that possibly correlate with the complex life cycle of streptomycetes. To see whether this was confined to the genus *Streptomyces*, we determined the phylogeny of SSB proteins by analysing representative SSBs from related orders of the phylum Actinobacteria. Phylogenetic analyses (Figure 8) revealed that SsbA and SsbB from orders Actinomycetales and Bifidobacteriales are clustered, indicating that duplication occurred in a common ancestor. Retention of paralogs in most members of these orders indicates that these gene products have well-established roles (48). Although the SsbB proteins are branched together, they evolved much faster, as indicated by branch lengths. In contrast, among SsbA proteins, homology is conserved, probably reflecting their essential biological role. In the case of SSBs from *S. nausensis* and *C. glutamicum*, the third SSB, SsbC could be the result of new duplication or it could be a consequence of recent horizontal transfer. Members of other analysed orders belong to the deepest branches of Actinobacteria (63). Interestingly, their clustering might indicate that some of them underwent recent duplication, as their SSBs were grouped together. Some genomes did not retain duplicated genes or duplication did not occur.

ACCESSION NUMBERS

PDB ID: 4DAM.

SUPLEMENTARY DATA

Supplementary Data are available at NAR Online: Supplementary Tables 1–4, Supplementary Figures 1–7 and Supplementary References [26,29,64–68].

ACKNOWLEDGEMENTS

The authors thank to D.A. Hopwood for critical review of the manuscript; to R. Kolter, H. Schrempf and J. Pigac for helpful comments; to I. Piantanida for his expert advice on fluorescence measurement analysis; to K.J. McDowall for sharing with us his unpublished results, to Z. Pedisic for statistical analysis and to A. Bielen and M. Paradzik for technical assistance in the manuscript preparation.

FUNDING

Croatian Ministry of Science, Education and Sports grant number [098-0982913-2877 to D.V. and 098-1191344-2943 to M.L.]. Also, the research leading to this publication has received funding from the European Community's Seventh Framework Programme (FP7/2007-2013) under grant agreement n.°[283570] (BioStruct-X). T.P. was the recipient of the short-term FEMS Research Fellowship in 2011 to visit the laboratory of PRH at the University of Strathclyde. Funding for open access charge: Croatian Ministry of Science, Education and Sports grant numbers: [098-0982913-2877 and 098-1191344-2943].

Conflict of interest statement. None declared.

REFERENCES

1. Hopwood,D.A. (1999) Forty years of genetics with Streptomyces: from in vivo through in vitro to in silico. *Microbiology*, **145(Pt 9)**, 2183–2202.
2. Bentley,S.D., Chater,K.F., Cerdeno-Tarraga,A.M., Challis,G.L., Thomson,N.R., James,K.D., Harris,D.E., Quail,M.A., Kieser,H., Harper,D. *et al.* (2002) Complete genome sequence of the model actinomycete Streptomyces coelicolor A3(2). *Nature*, **417**, 141–147.
3. Szczepankowska,A.K., Prestel,E., Mariadassou,M., Bardowski,J.K. and Bidnenko,E. (2011) Phylogenetic and complementation analysis of a single-stranded DNA binding protein family from lactococcal phages indicates a non-bacterial origin. *PLoS One*, **6**, e26942.
4. Meyer,R.R. and Laine,P.S. (1990) The single-stranded DNA-binding protein of Escherichia coli. *Microbiol. Rev.*, **54**, 342–380.
5. Glassberg,J., Meyer,R.R. and Kornberg,A. (1979) Mutant single-strand binding protein of *Escherichia coli*: genetic and physiological characterization. *J. Bacteriol.*, **140**, 14–19.
6. Shereda,R.D., Kozlov,A.G., Lohman,T.M., Cox,M.M. and Keck,J.L. (2008) SSB as an organizer/mobilizer of genome maintenance complexes. *Crit. Rev. Biochem. Mol. Biol.*, **43**, 289–318.
7. Costes,A., Lecointe,F., McGovern,S., Quevillon-Cheruel,S. and Polard,P. (2010) The C-terminal domain of the bacterial SSB protein acts as a DNA maintenance hub at active chromosome replication forks. *PLoS Genet.*, **6**, e1001238.
8. Murzin,A.G. (1993) OB(oligonucleotide/oligosaccharide binding)-fold: common structural and functional solution for non-homologous sequences. *EMBO J.*, **12**, 861–867.
9. Curth,U., Genschel,J., Urbanke,C. and Greipel,J. (1996) In vitro and in vivo function of the C-terminus of Escherichia coli single-stranded DNA binding protein. *Nucleic Acids Res.*, **24**, 2706–2711.
10. Raghunathan,S., Ricard,C.S., Lohman,T.M. and Waksman,G. (1997) Crystal structure of the homo-tetrameric DNA binding domain of Escherichia coli single-stranded DNA-binding protein determined by multiwavelength x-ray diffraction on the selenomethionyl protein at 2.9-A resolution. *Proc. Natl Acad. Sci. USA*, **94**, 6652–6657.
11. Stefanic,Z., Vujaklija,D. and Luic,M. (2009) Structure of the single-stranded DNA-binding protein from Streptomyces coelicolor. *Acta. Crystallogr. D Biol. Crystallogr.*, **65**, 974–979.
12. Roy,R., Kozlov,A.G., Lohman,T.M. and Ha,T. (2007) Dynamic structural rearrangements between DNA binding modes of *E. coli* SSB protein. *J. Mol. Biol.*, **369**, 1244–1257.
13. Lindner,C., Nijland,R., van Hartskamp,M., Bron,S., Hamoen,L.W. and Kuipers,O.P. (2004) Differential expression of two paralogous genes of *Bacillus subtilis* encoding single-stranded DNA binding protein. *J. Bacteriol.*, **186**, 1097–1105.
14. Yadav,T., Carrasco,B., Myers,A.R., George,N.P., Keck,J.L. and Alonso,J.C. (2012) Genetic recombination in *Bacillus subtilis*: a division of labor between two single-strand DNA-binding proteins. *Nucleic Acids Res.*, **40**, 5546–5559.
15. Grove,D.E., Willcox,S., Griffith,J.D. and Bryant,F.R. (2005) Differential single-stranded DNA binding properties of the paralogous SsbA and SsbB proteins from *Streptococcus pneumoniae*. *J. Biol. Chem.*, **280**, 11067–11073.
16. Flardh,K., Richards,D.M., Hempel,A.M., Howard,M. and Buttner,M.J. (2012) Regulation of apical growth and hyphal branching in *Streptomyces*. *Curr. Opin. Microbiol.*, **15**, 737–743.
17. Ruban-Osmialowska,B., Jakimowicz,D., Smulczyk-Krawczyszyn,A., Chater,K.F. and Zakrzewska-Czerwinska,J. (2006) Replisome localization in vegetative and aerial hyphae of *Streptomyces coelicolor*. *J. Bacteriol.*, **188**, 7311–7316.
18. Flardh,K. and Buttner,M.J. (2009) Streptomyces morphogenetics: dissecting differentiation in a filamentous bacterium. *Nat. Rev. Microbiol.*, **7**, 36–49.
19. Jakimowicz,D. and van Wezel,G.P. (2012) Cell division and DNA segregation in Streptomyces: how to build a septum in the middle of nowhere? *Mol. Microbiol.*, **85**, 393–404.
20. Wang,L., Yu,Y., He,X., Zhou,X., Deng,Z., Chater,K.F. and Tao,M. (2007) Role of an FtsK-like protein in genetic stability in Streptomyces coelicolor A3(2). *J. Bacteriol.*, **189**, 2310–2318.
21. Dedrick,R.M., Wildschutte,H. and McCormick,J.R. (2009) Genetic interactions of smc, ftsK, and parB genes in Streptomyces coelicolor and their developmental genome segregation phenotypes. *J. Bacteriol.*, **191**, 320–332.
22. Kois,A., Swiatek,M., Jakimowicz,D. and Zakrzewska-Czerwinska,J. (2009) SMC protein-dependent chromosome condensation during aerial hyphal development in Streptomyces. *J. Bacteriol.*, **191**, 310–319.
23. Kim,H.J., Calcutt,M.J., Schmidt,F.J. and Chater,K.F. (2000) Partitioning of the linear chromosome during sporulation of *Streptomyces coelicolor* A3(2) involves an oriC-linked parAB locus. *J. Bacteriol.*, **182**, 1313–1320.
24. Jakimowicz,D., Zydek,P., Kois,A., Zakrzewska-Czerwinska,J. and Chater,K.F. (2007) Alignment of multiple chromosomes along helical ParA scaffolding in sporulating *Streptomyces hyphae*. *Mol. Microbiol.*, **65**, 625–641.
25. Ditkowski,B., Troc,P., Ginda,K., Donczew,M., Chater,K.F., Zakrzewska-Czerwinska,J. and Jakimowicz,D. (2010) The actinobacterial signature protein ParJ (SCO1662) regulates ParA polymerization and affects chromosome segregation and cell division during *Streptomyces sporulation*. *Mol. Microbiol.*, **78**, 1403–1415.
26. Pigac,J. and Schrempf,H. (1995) A simple and rapid method of transformation of *Streptomyces rimosus* r6 and other streptomycetes by electroporation. *Appl. Environ. Microbiol.*, **61**, 352–356.
27. Kieser,T.B., Buttner,M.J., Chater,K.F. and Hopwood,D.A. (2000) *Practical Streptomyces Genetics*. The John Innes Foundation, Norwich.
28. Mijakovic,I., Petranovic,D., Macek,B., Cepo,T., Mann,M., Davies,J., Jensen,P.R. and Vujaklija,D. (2006) Bacterial single-stranded DNA-binding proteins are phosphorylated on tyrosine. *Nucleic Acids Res.*, **34**, 1588–1596.
29. Waters,B., Vujaklija,D., Gold,M.R. and Davies,J. (1994) Protein tyrosine phosphorylation in streptomycetes. *FEMS Microbiol. Lett.*, **120**, 187–190.
30. Fernandez-Martinez,L.T., Del Sol,R., Evans,M.C., Fielding,S., Herron,P.R., Chandra,G. and Dyson,P.J. (2011) A transposon insertion single-gene knockout library and new ordered cosmid library for the model organism Streptomyces coelicolor A3(2). *Antonie Van Leeuwenhoek*, **99**, 515–522.
31. Gust,B., Chandra,G., Jakimowicz,D., Yuqing,T., Bruton,C.J. and Chater,K.F. (2004) Lambda red-mediated genetic manipulation of antibiotic-producing *Streptomyces*. *Adv. Appl. Microbiol.*, **54**, 107–128.
32. Schwedock,J., McCormick,J.R., Angert,E.R., Nodwell,J.R. and Losick,R. (1997) Assembly of the cell division protein FtsZ into ladder-like structures in the aerial hyphae of *Streptomyces coelicolor*. *Mol. Microbiol.*, **25**, 847–858.
33. Jyothikumar,V., Klanbut,K., Tiong,J., Roxburgh,J.S., Hunter,I.S., Smith,T.K. and Herron,P.R. (2012) Cardiolipin synthase is required for *Streptomyces coelicolor* morphogenesis. *Mol. Microbiol.*, **84**, 181–197.
34. Otwinowski,Z. and Minor,W. (1997) Processing of X-ray diffraction data collected in oscillation mode. *Macromol. Crystallogr.*, **276(Pt A)**, 307–326.
35. Kissinger,C.R., Gehlhaar,D.K. and Fogel,D.B. (1999) Rapid automated molecular replacement by evolutionary search. *Acta. Crystallogr. D Biol. Crystallogr.*, **55**, 484–491.
36. Langer,G., Cohen,S.X., Lamzin,V.S. and Perrakis,A. (2008) Automated macromolecular model building for X-ray crystallography using ARP/wARP version 7. *Nat. Protoc.*, **3**, 1171–1179.
37. Emsley,P. and Cowtan,K. (2004) Coot: model-building tools for molecular graphics. *Acta. Crystallogr. D Biol. Crystallogr.*, **60**, 2126–2132.
38. Murshudov,G.N., Vagin,A.A. and Dodson,E.J. (1997) Refinement of macromolecular structures by the maximum-likelihood method. *Acta. Crystallogr. D Biol. Crystallogr.*, **53**, 240–255.
39. McGhee,J.D. and von Hippel,P.H. (1974) Theoretical aspects of DNA-protein interactions: co-operative and non-co-operative

binding of large ligands to a one-dimensional homogeneous lattice. *J. Mol. Biol.*, **86**, 469–489.
40. Klotz,I.M. (1997) *Ligand-receptor energetics:a guide for the perplexed*. Wiley, New York.
41. Heichlinger,A., Ammelburg,M., Kleinschnitz,E.M., Latus,A., Maldener,I., Flardh,K., Wohlleben,W. and Muth,G. (2011) The MreB-like protein Mbl of *Streptomyces coelicolor* A3(2) depends on MreB for proper localization and contributes to spore wall synthesis. *J. Bacteriol.*, **193**, 1533–1542.
42. Pei,J. and Grishin,N.V. (2007) PROMALS: towards accurate multiple sequence alignments of distantly related proteins. *Bioinformatics*, **23**, 802–808.
43. Abascal,F., Zardoya,R. and Posada,D. (2005) ProtTest: selection of best-fit models of protein evolution. *Bioinformatics*, **21**, 2104–2105.
44. Guindon,S., Dufayard,J.F., Lefort,V., Anisimova,M., Hordijk,W. and Gascuel,O. (2010) New algorithms and methods to estimate maximum-likelihood phylogenies: assessing the performance of PhyML 3.0. *Syst. Biol.*, **59**, 307–321.
45. Anisimova,M. and Gascuel,O. (2006) Approximate likelihood-ratio test for branches: A fast, accurate, and powerful alternative. *Syst. Biol.*, **55**, 539–552.
46. Gouy,M., Guindon,S. and Gascuel,O. (2010) SeaView version 4: A multiplatform graphical user interface for sequence alignment and phylogenetic tree building. *Mol. Biol. Evol.*, **27**, 221–224.
47. Marintcheva,B., Marintchev,A., Wagner,G. and Richardson,C.C. (2008) Acidic C-terminal tail of the ssDNA-binding protein of bacteriophage T7 and ssDNA compete for the same binding surface. *Proc. Natl Acad. Sci. USA*, **105**, 1855–1860.
48. Bratlie,M.S., Johansen,J., Sherman,B.T., Huang da,W., Lempicki,R.A. and Drablos,F. (2010) Gene duplications in prokaryotes can be associated with environmental adaptation. *BMC Genomics*, **11**, 588.
49. Jakimowicz,D., Mouz,S., Zakrzewska-Czerwinska,J. and Chater,K.F. (2006) Developmental control of a parAB promoter leads to formation of sporulation-associated ParB complexes in *Streptomyces coelicolor*. *J. Bacteriol.*, **188**, 1710–1720.
50. Ryding,N.J., Bibb,M.J., Molle,V., Findlay,K.C., Chater,K.F. and Buttner,M.J. (1999) New sporulation loci in *Streptomyces coelicolor* A3(2). *J. Bacteriol.*, **181**, 5419–5425.
51. Ainsa,J.A., Ryding,N.J., Hartley,N., Findlay,K.C., Bruton,C.J. and Chater,K.F. (2000) WhiA, a protein of unknown function conserved among gram-positive bacteria, is essential for sporulation in *Streptomyces coelicolor* A3(2). *J. Bacteriol.*, **182**, 5470–5478.
52. Bourn,W.R. and Babb,B. (1995) Computer assisted identification and classification of streptomycete promoters. *Nucleic Acids Res.*, **23**, 3696–3703.
53. Strohl,W.R. (1992) Compilation and analysis of DNA sequences associated with apparent streptomycete promoters. *Nucleic Acids Res.*, **20**, 961–974.
54. Ahel,I., Vujaklija,D., Mikoc,A. and Gamulin,V. (2002) Transcriptional analysis of the recA gene in Streptomyces rimosus: identification of the new type of promoter. *FEMS Microbiol. Lett.*, **209**, 133–137.
55. Krissinel,E. and Henrick,K. (2004) Secondary-structure matching (SSM), a new tool for fast protein structure alignment in three dimensions. *Acta. Crystallogr. D Biol. Crystallogr.*, **60**, 2256–2268.
56. Krissinel,E. and Henrick,K. (2007) Inference of macromolecular assemblies from crystalline state. *J. Mol. Biol.*, **372**, 774–797.
57. Stefanic,Z., Vujaklija,D., Andrisic,L., Mikleusevic,G., Andrejasic,M., Turk,D. and Luic,M. (2007) Preliminary crystallographic study of *Streptomyces coelicolor* single-stranded DNA-binding protein. *Croatica. Chemica. Acta.*, **80**, 35–39.
58. Noens,E.E., Mersinias,V., Traag,B.A., Smith,C.P., Koerten,H.K. and van Wezel,G.P. (2005) SsgA-like proteins determine the fate of peptidoglycan during sporulation of *Streptomyces coelicolor*. *Mol. Microbiol.*, **58**, 929–944.
59. Flardh,K., Findlay,K.C. and Chater,K.F. (1999) Association of early sporulation genes with suggested developmental decision points in *Streptomyces coelicolor* A3(2). *Microbiology*, **145(Pt 9)**, 2229–2243.
60. Kang,J.G., Paget,M.S., Seok,Y.J., Hahn,M.Y., Bae,J.B., Hahn,J.S., Kleanthous,C., Buttner,M.J. and Roe,J.H. (1999) RsrA, an anti-sigma factor regulated by redox change. *EMBO J.*, **18**, 4292–4298.
61. Lohman,T.M. and Ferrari,M.E. (1994) Escherichia coli single-stranded DNA-binding protein: multiple DNA-binding modes and cooperativities. *Annu. Rev. Biochem.*, **63**, 527–570.
62. Kozlov,A.G., Cox,M.M. and Lohman,T.M. (2010) Regulation of single-stranded DNA binding by the C termini of *Escherichia coli* single-stranded DNA-binding (SSB) protein. *J. Biol. Chem.*, **285**, 17246–17252.
63. Zhi,X.Y., Li,W.J. and Stackebrandt,E. (2009) An update of the structure and 16S rRNA gene sequence-based definition of higher ranks of the class Actinobacteria, with the proposal of two new suborders and four new families and emended descriptions of the existing higher taxa. *Int. J. Syst. Evol. Microbiol.*, **59**, 589–608.
64. Gust,B., Challis,G.L., Fowler,K., Kieser,T. and Chater,K.F. (2003) PCR-targeted Streptomyces gene replacement identifies a protein domain needed for biosynthesis of the sesquiterpene soil odor geosmin. *Proc. Natl Acad. Sci. USA*, **100**, 1541–1546.
65. Gregory,M.A., Till,R. and Smith,M.C. (2003) Integration site for Streptomyces phage phiBT1 and development of site-specific integrating vectors. *J. Bacteriol.*, **185**, 5320–5323.
66. DeSanti,C.L. and Strohl,W.R. (2003) Characterization of the *Streptomyces sp.* strain C5 snp locus and development of snp-derived expression vectors. *Appl. Environ. Microbiol.*, **69**, 1647–1654.
67. MacNeil,D.J., Gewain,K.M., Ruby,C.L., Dezeny,G., Gibbons,P.H. and MacNeil,T. (1992) Analysis of *Streptomyces avermitilis* genes required for avermectin biosynthesis utilizing a novel integration vector. *Gene*, **111**, 61–68.
68. Cherepanov,P.P. and Wackernagel,W. (1995) Gene disruption in *Escherichia coli*: TcR and KmR cassettes with the option of Flp-catalyzed excision of the antibiotic-resistance determinant. *Gene*, **158**, 9–14.